Inorg. Chem. **2009**, *48*, 2639−2651

Interactions of a Cationic Mercury(II) Thiolate Complex $[Hg(Tab)_2](PF_6)_2$ with N-Donor Ligands

Xiao-Yan Tang,[†,‡] Rong-Xin Yuan,[§] Zhi-Gang Ren,[†] Hong-Xi Li,[†] Yong Zhang,[†] and Jian-Ping Lang*[,†,‡]

Key Laboratory of Organic Synthesis of Jiangsu Province, College of Chemistry, Chemical Engineering and Materials Science, Suzhou University, Suzhou 215123, People's Republic of China, State Key Laboratory of Organometallic Chemistry, Shanghai Institute of Organic Chemistry, Chinese Academy of Sciences, Shanghai 210093, People's Republic of China, and Jiangsu Laboratory of Advanced Functional Materials, Changshu Institute of Technology, Changshu 215500, People's Republic of China

Received November 12, 2008

Reactions of $[Hg(Tab)_2](PF_6)_2$ (**1**) with phen, 2,2′-bipy, py, N-Meim, N-^{i}Prim, en, eten, tmen, dap, and dpt gave rise to a family of cationic mercury(II) thiolate complexes, $[Hg(Tab)_2(L)](PF_6)_2 \cdot S$ (**2**, L = phen, S = 2MeOH; **3**, L = 2,2′-bipy, S = DMF), $[Hg(Tab)_2(L)_2](PF_6)_2$ (**4**, L = py; **5**, L = N-Meim), $[Hg(Tab)_2(N\text{-}^i\text{Prim})](PF_6)_2$ (**6**), $[Hg(Tab)_2(L)](PF_6)_2 \cdot 0.5MeCN$ (**7**, L = en; **8**, L = eten), and $[Hg(Tab)_2(L)](PF_6)_2$ (**9**, L = tmen; **10**, L = dap; **11**, L = dpt). These complexes were characterized by elemental analysis, IR spectra, UV−vis spectra, ^{1}H NMR, and single-crystal X-ray crystallography. The Hg atom in $[Hg(Tab)_2]^{2+}$ dications of **2**−**5** is further coordinated either by two N atoms from one phen or 2,2′-bipy ligand or by two N atoms from two py or N-Meim ligands, affording a distorted seesaw-shaped coordination geometry. In **6**, the Hg atom of the $[Hg(Tab)_2]^{2+}$ dication is coordinated by one N atom of the N-^{i}Prim ligand, forming a T-shaped coordination geometry, and these $[Hg(Tab)_2(N\text{-}^i\text{Prim})]^{2+}$ dications are further coordinated to another S atom of Tab from the adjacent unit, giving a chain structure. The Hg atoms in $[Hg(Tab)_2]^{2+}$ dications of **7**−**11** are chelated by two N atoms from one diamine molecule such as en in **7**, eten in **8**, tmen in **9**, or dap in **10** or by two N atoms from the triamine molecule dpt in **11**, forming a distorted seesaw-shaped coordination geometry. In all of these structures, the original trans configuration of the $[Hg(Tab)_2]^{2+}$ dication of **1** is changed via rotation and/or switching of the two Tab species along the S−Hg−S line together with the rotation of the phenyl groups of the Tab ligands. The results may provide interesting insight into mimicking of the interactions of the $Hg(Cys)_2$ linear species in Hg-MerR and Hg-MT with various N-donor ligands encountered in nature and its potential changes in the structural chemistry (bond length, angles, configurations, etc.).

Introduction

Immense interest in the coordination chemistry of mercury thiolate complexes continues to be motivated by the importance of these complexes as structural models in the detoxification of mercury by metallothioneins (MTs),[1] in DNA binding proteins,[2] and in the mercury reductase and related proteins.[3] Among these complexes, monomeric mercury−cysteine (Hg-Cys) coordination centers have been implicated for the proteins involved in bacterial mercury detoxification, which include mercuric ion reductase, organomercury lyase, and metalloregulatory protein (MerR).[4]These biological problems have encouraged interest in the characterization of monomeric Hg-Cys complexes.[5] In the structures of Hg-MerR and Hg-MT, the geometry for the Hg centers was assumed to be two-, three-, or four-coordinated.[4c,6] Although distorted four-coordinated environments were also suggested for some other Hg-substituted proteins based on the existence of low-energy UV transitions, those assignments were not confirmed by comparison with those of the mononuclear complexes $[Hg(SR)_n]^{x-}$ (n = 3, 4; x = 1, 2).[7a−d] O'Halloran et al. suggested that the primary coordination environments corresponding to $[HgS_2N_n]$ (n = 1, 2) in these proteins might be taken into account because of the absence of

* To whom correspondence should be addressed. E-mail: jplang@suda.edu.cn.
† Suzhou University.
‡ Chinese Academy of Sciences.
§ Changshu Institute of Technology.

10.1021/ic8021744 CCC: $40.75
Published on Web 02/19/2009

spectroscopic data on the model compounds.[7a] To our knowledge, studies on the introduction of the N-donor ligands into the linear mercury thiolate model complexes and the subsequent structural variations of the resulting $[HgS_2N_n]$ complexes seem to be less explored.[8]

Recently, we have been engaged in the preparation of metal complexes of a zwitterionic thiolate, 4-(trimethylammonio)benzenethiol (TabH). This ligand bears an ammonium group and a sulfhydryl group and to some extent is similar to cysteine. Among those metal/Tab complexes isolated,[9] the mononuclear mercury(II) complex $[Hg(Tab)_2](PF_6)_2$ (**1**) could be used as a model complex in mimicking the reactivity of the unsaturated HgS_2 species in Hg-MerR and Hg-MT. Previous results revealed that **1** did interact with some donor ligands (e.g., Tab, NCS^-, I^-)[9c] and inorganic anions (e.g., Cl^-, NO_2^-, NO_3^-).[9f] In most of these reactions, the linear coordination geometry of the Hg atom in **1** was further fulfilled by additional donor ligands. On the other hand, it is known that the N atoms of pyridine,[10a] imidazole[10b−d] or purine derivatives,[10e−g] or alkylamine ligands (e.g., ethyldiamine,[11a−c] propyldiamine,[11d] and diethylenetriamine[2c,11e]) have some affinity for the unsaturated mercury. Such an interaction between Hg and N-donor ligands might be of importance. For example, when DNA was readily denatured by methylmercury,[12] interactions of the imidazole moiety with methylmercury might provide one pathway to mercury poisoning.[10b] Considering that N-heterocyclic compounds and alkylamines are always encountered in nature, we deliberately selected five N-heterocyclic compounds and five alkylamines (Chart 1) as N-donor ligands to react with **1**, and a family of cationic adduct complexes $[Hg(Tab)_2L_n](PF_6)_2$ (**2**−**11**; L = N-donor ligand, n = 1, 2) were isolated therefrom (Chart 2). Herein we report the interactions of **1** with these N-donor ligands along with the isolation and characterization of **2**−**11**. The results are part of a systematic study of the model complex **1** with N-donor ligands, aiming to provide a basis for a better understanding of the reactivity and structural variations of the HgS_2 species in Hg-MerR and Hg-MT.

Chart 1. Structures of phen, 2,2′-bipy, py, N-Meim, N-^{i}Prim, en, eten, tmen, dap, and dpt Ligands

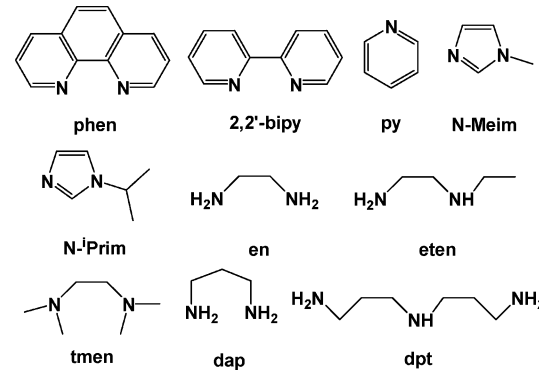

Chart 2. Designations of Compounds and Abbreviations[a] of **2**−**11**

$[Hg(Tab)_2](PF_6)_2$ (**1**)[9c]

$[Hg(Tab)_2(L)](PF_6)_2 \cdot S$ (**2**, L = phen, S = 2MeOH; **3**, L = 2,2′-bipy, S = DMF)

$[Hg(Tab)_2(L)_2](PF_6)_2$ (**4**, L = py; **5**, L = N-Meim)

$[Hg(Tab)_2(N\text{-}^iPrim)](PF_6)_2$ (**6**)

$[Hg(Tab)_2(L)](PF_6)_2 \cdot 0.5MeCN$ (**7**, L = en; **8**, L = eten)

$[Hg(Tab)_2(L)](PF_6)_2$ (**9**, L = tmen; **10**, L = dap; **11**, L = dpt)

[a] Tab = 4-(trimethylammonio)benzenethiolate; phen = phenanthroline; 2,2′-bipy = 2,2′-bipyridine; py = pyridine; N-Meim = *N*-methylimidazole; N-^{i}Prim = *N*-isopropylimidazole; en = 1,2-diaminoethane; eten = *N*-ethyl-1,2-diaminoethane; tmen = *N*,*N*,*N*′,*N*′-tetramethyl-1,2-diaminoethane; dap = 1,3-diaminopropane; dpt = dipropylenetriamine.

(1) (a) Fleischer, H.; Dienes, Y.; Mathiasch, B.; Schmitt, V.; Schollmeyer, D. *Inorg. Chem.* **2005**, *44*, 8087. (b) Wright, J. G.; Natan, M. J.; MacDonnell, F. M.; Ralston, D. M.; O'Halloran, T. V. *Prog. Inorg. Chem.* **1990**, *38*, 323. (c) Baba, K.; Okamura, T.; Yamamoto, H.; Yamamoto, T.; Ueyama, N. *Inorg. Chem.* **2008**, *47*, 2837. (d) Vig, K.; Megharaj, M.; Sethunathan, N.; Naidu, R. *Adv. Environ. Res.* **2003**, *8*, 121. (e) Sigel, A.; Sigel, H. In Metal Ions in Biological Chemical Toxicology and Clinical Chemistry of Metals; Brown, S. S., Savoy, J., Eds.; Dekker: New York, 1997. (f) Stillman, M. J.; Law, A. Y. C.; Szymanska, J. A. In *Chemical Toxicology and Clinical Chemistry of Metals*; Brown, S. S., Savoy, J., Eds.; Academic: London, 1983; p 275.

(2) (a) Kuklenyik, Z.; Marzilli, L. G. *Inorg. Chem.* **1996**, *35*, 5654. (b) Utschig, L. M.; Wright, J. G.; O'Halloran, T. *Methods Enzymol.* **1993**, *226*, 71. (c) Patra, G. K.; Goldberg, I. *Polyhedron* **2002**, *21*, 2195. (d) Dance, I. G. *Polyhedron* **1986**, *5*, 1037. (e) Henkel, G.; Krebs, B. *Chem. Rev.* **2004**, *104*, 801. (f) Engst, S.; Miller, S. M. *Biochemistry* **1999**, *38*, 3519.

(3) (a) Bharara, M. S.; Bui, T. H.; Parkin, S.; Atwood, D. A. *J. Chem. Soc., Dalton Trans.* **2005**, 3874. (b) Blower, P. J.; Dilworth, J. R. *Coord. Chem. Rev.* **1987**, *76*, 121. (c) Bharara, M. S.; Parkin, S.; Atwood, D. A. *Inorg. Chem.* **2006**, *45*, 7261. (d) Wright, J. G.; Natan, M. J.; MacDonnell, F. M.; Ralston, D. M.; O'Halloran, T. V. *Mercury(II)-Thiolate Chemistry and the Mechanism of the Heavy Metal Biosensor MerR*; John Wiley & Sons: New York, 1990. (e) Stillman, M. J., Shaw, C. F., Suzuki, K. T., Eds. *Metallothioneins: Synthesis, Structure and Properties of Metallothioneins, Phytochelatins and Metal-Thiolate Complexes*; John Wiley & Sons: New York, 1992. (f) Chan, J.; Huang, Z. Y.; Merrifield, M. E.; Salgado, M. T.; Stillman, M. J. *Coord. Chem. Rev.* **2002**, *233*−*234*, 319. (g) Qian, H.; Sahlman, L.; Eriksson, P. O.; Hambraeus, C.; Edlund, U.; Sethson, I. *Biochemistry* **1998**, *37*, 9316.

(4) (a) Moore, M. J.; Distefano, M. D.; Zydowsky, L. D.; Cummings, R. T.; Walsh, C. T. *Acc. Chem. Res.* **1990**, *23*, 301. (b) Ralston, D. M.; O'Halloran, T. V. *Adv. Inorg. Biochem.* **1990**, *8*, 1. (c) Gruff, E. S.; Koch, S. A. *J. Am. Chem. Soc.* **1990**, *112*, 1245. (d) Helmann, J. D.; Shewchuk, L. M.; Walsh, C. T. *Adv. Inorg. Biochem.* **1990**, *8*, 33. (e) Govindaswamy, N.; Moy, J.; Millar, M.; Koch, S. A. *Inorg. Chem.* **1992**, *31*, 5343.

(5) (a) Natan, M. J.; Millikan, C. F.; Wright, J. G.; O'Halloran, T. V. *J. Am. Chem. Soc.* **1990**, *112*, 3255. (b) Santos, R. A.; Gruff, E. S.; Koch, S. A.; Harbison, G. S. *J. Am. Chem. Soc.* **1991**, *113*, 469.

(6) (a) Shewchuk, L. M.; Verdine, G. L.; Nash, H.; Walsh, C. T. *Biochemistry* **1989**, *28*, 6140. (b) O'Halloran, T. V.; Frantz, B.; Shin, M. K.; Ralston, D. M.; Wright, J. G. *Cell* **1989**, *56*, 119. (c) Penner-Hahn, J. E.; Tsang, H. T.; O'Halloran, T. V.; Wright, J. *Physica B* **1989**, *158*, 117. (d) Steele, R. A.; Opella, S. J. *Biochemistry* **1997**, *36*, 6885. (e) Veglia, G.; Porcelli, F.; Desilva, T.; Prantner, A.; Opella, S. J. *J. Am. Chem. Soc.* **2000**, *122*, 2389. (f) Silver, A.; Koch, S. A.; Millar, M. *Inorg. Chim. Acta* **1993**, *9*, 205. (g) Choudhury, S.; Dance, I. G.; Guerney, P.; Rae, A. D. *Inorg. Chim. Acta* **1983**, *70*, 227. (h) Christou, G.; Folting, K.; Huffmann, J. C. *Polyhedron* **1984**, *3*, 1247. (i) Lavertue, P.; Hubert, J.; Beauchamp, A. L. *Inorg. Chem.* **1976**, *15*, 322. (j) Bowmaker, G. A.; Dance, I. G.; Harris, R. K.; Henderson, W.; Laban, I.; Scudder, M. L.; Oh, S. W. *J. Chem. Soc., Dalton Trans.* **1996**, *11*, 2381. (k) Shewchuk, L. M.; Verdine, G. L.; Walsh, C. T. *Biochemistry* **1989**, *28*, 2331. (l) Raybuck, S. A.; Distefano, M. D.; Teo, B. K.; Orme-Johnson, W.; Walsh, C. T. *J. Am. Chem. Soc.* **1990**, *112*, 1983. (m) Helmann, J. D.; Ballard, B. T.; Walsh, C. T. *Science* **1990**, *247*, 946. (n) Moore, M. J.; Distefano, M. D.; Walsh, C. T.; Schiering, N.; Pai, E. F. *J. Biol. Chem.* **1989**, *264*, 14386. (o) Lu, W. H.; Zelazowski, A. J.; Stillman, M. J. *Inorg. Chem.* **1993**, *32*, 919.

(7) (a) Watton, S. P.; Wright, J. G.; MacDonnell, F. M.; Bryson, J. W.; Sabat, M.; O'Halloran, T. V. *J. Am. Chem. Soc.* **1990**, *112*, 2824. (b) Vasak, M.; Kaegi, J. H. R.; Hill, H. A. O. *Biochemistry* **1981**, *20*, 2852. (c) Johnson, B. A.; Armitage, I. M. *Inorg. Chem.* **1987**, *26*, 3139. (d) Tamilarasan, R.; McMillin, D. R. *Inorg. Chem.* **1986**, *25*, 2037.

Scheme 1. Reactions of **1** with phen, 2,2′-bipy, py, N-Meim, and N-^{i}Prim Ligands

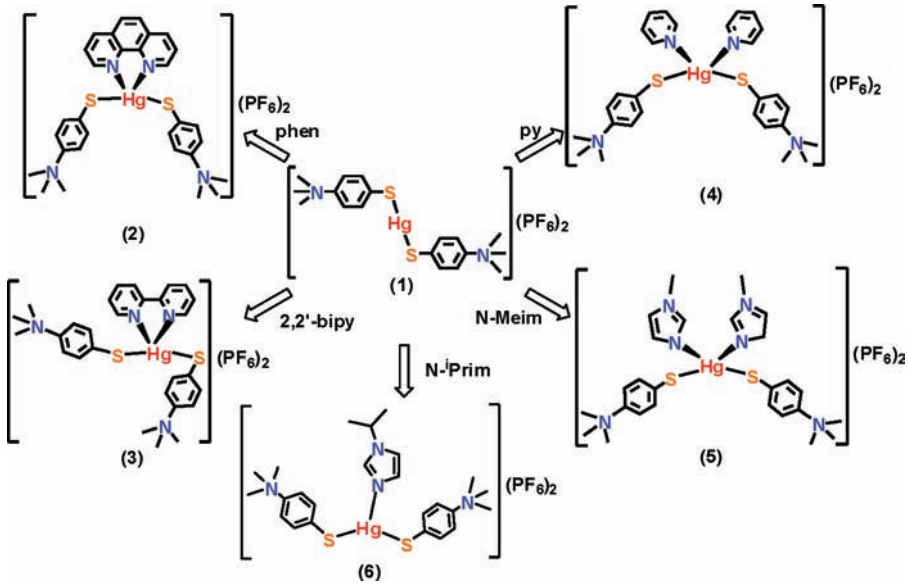

Scheme 2. Reactions of **1** with en, eten, tmen, dap, and dpt Ligands

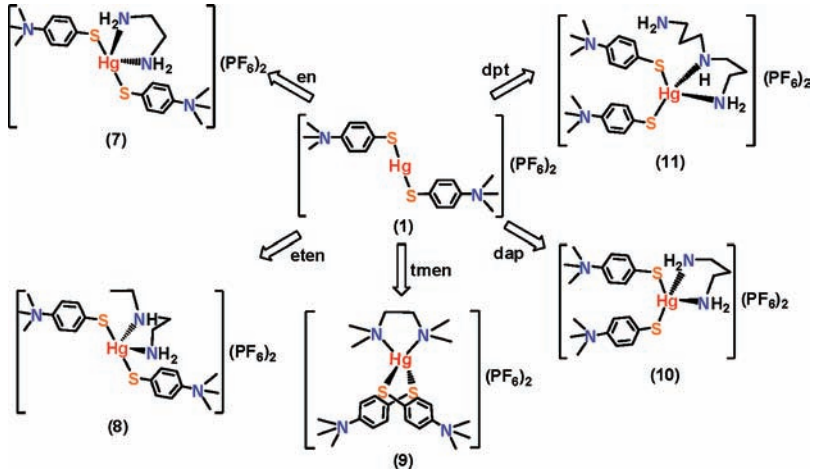

Results and Discussion

Synthetic and Spectral Aspects. Because the linear coordination geometry of the central Hg atom in **1** can be saturated by up to two donor ligands, reactions of **1** with N-heterocyclic ligands and alkylamine ligands are anticipated to yield 1:1 or 1:2 adduct complexes depending on the number of donor atoms in these ligands. Therefore, treatment of **1** with 1 or 2 equiv of phen or 2,2′-bipy in MeOH/H_2O gave rise to the mononuclear 1:1 adduct complex **2** or **3** in an almost quantitative yield (Scheme 1). When **1** reacted with a slight excess of pyridine or N-Meim, it afforded the expected 1:2 adduct complexes **4** and **5** in high yields. Analogous reactions with different **1**-to-L (L = N-donor ligand) molar ratios always yielded the same products. However, similar reactions of **1** with 2 equiv of N-^{i}Prim did not produce the expected 1:2 adduct $[Hg(Tab)_2(N\text{-}^{i}Prim)_2](PF_6)_2$ but a 1:1 adduct **6** in 90% yield.

On the other hand, reactions of **1** with 2 equiv of alkyldiamine ligands such as en, eten, tmen, and dap in MeOH led to the formation of the corresponding 1:1 mononuclear adduct complexes **7** (85% yield), **8** (83% yield), **9** (82% yield), and **10** (87% yield), respectively (Scheme 2). In the case of alkyltriamine ligand dpt, we initially attempted this ligand to prepare a polynuclear Hg/Tab/dpt complex. However, treatment of **1** with dpt followed by a standard workup only afforded a mononuclear complex **11**. As described later in this paper, the third amine group of dpt in **11** did not bind to the central Hg or other Hg centers.

Compounds **2**−**11** were stable toward oxygen and moisture, readily soluble in DMSO, DMF, and MeCN, and insoluble in MeOH, EtOH, CH_2Cl_2, benzene, and H_2O. The elemental analyses were consistent with their chemical formulas. The IR spectra for **2**−**11** are quite similar to that of **1** except the peaks around 3000−3400 cm^{-1} that are involved in the symmetric and asymmetric N−H stretching

(8) (a) Popovic, Z.; Soldin, Z.; Pavlovic, G.; Matkovic-Calogovic, D.; Mrvos-Sermek, D.; Rajic, M. *Struct. Chem.* **2002**, *13*, 425. (b) Bochmann, M.; Webb, K. J.; Powell, A. K. *Polyhedron* **1992**, *11*, 513.

vibrations[13] for the primary and secondary amines in **7**, **8**, **10**, and **11**. In the case of **7** and **10**, the sharp bands at 3376/3310 cm^{-1} (**7**) or 3370/3307 cm^{-1} (**10**) can be assigned to be the symmetric and asymmetric N−H stretching vibrations of the chelated NH_2 groups of the en or dap ligand. In the IR spectra of **8** and **11**, two weak υ(N−H) bands at ca. 3372/3325 cm^{-1} (**8**) and 3375/3310 cm^{-1} (**11**) are somewhat broad compared with those of **7** and **10**. It is assumed that the N−H stretching vibrations of the chelated NH group may be overlapped with those of the chelated NH_2 group and the free NH_2 group in the case of **11**. Besides, the characteristic P−F stretching vibrations of PF_6^- at ca. 838 and 558 cm^{-1} were all observed in the IR spectra of **2**−**11**. The ^{1}H NMR spectra of **2**−**11** in $(CD_3)_2SO$ at ambient temperature feature multiplets in the region of 7.34−7.73 ppm for phenyl groups of the Tab ligands and a singlet at ca. 3.52 ppm for the methyl protons of the NMe_3 units. For **2**−**6**, a set of peaks related to phen (**2**), 2,2′-bipy (**3**), py (**4**), N-Meim (**5**), and N-^{i}Prim (**6**) are also observed. Signals for the amine protons appear at 3.15 ppm in **7**, 3.43 ppm in **8**, 3.23 ppm in **10**, and 3.48 ppm in **11**. Other resonances in the ^{1}H NMR spectra of **7**−**11** are assigned as follows: multiplets at 2.64 (**7**), 2.38−2.73 (**8**), 2.48 (**9**), 2.75 and 1.48−1.53 (**10**), and 3.45 (**11**) ppm for methylene protons of the diamine or triamine ligands, singlets at 2.28 (**9**) ppm for the methyl protons of eten, and multiplets in the region of 1.03−1.06 (**8**) ppm for the methyl protons of tmen.

The electronic spectra of **2**−**11** in MeCN exhibit strong and broad absorptions ranging from 256 to 280 nm and a long absorption tail at ca. 400 nm (Figure 1). Compared to the broad absorption band at 314 nm of the Tab ligand in MeCN,[9c] those main absorption bands observed in the spectra of **2**−**11** are blue-shifted and may be ascribed to the ligand

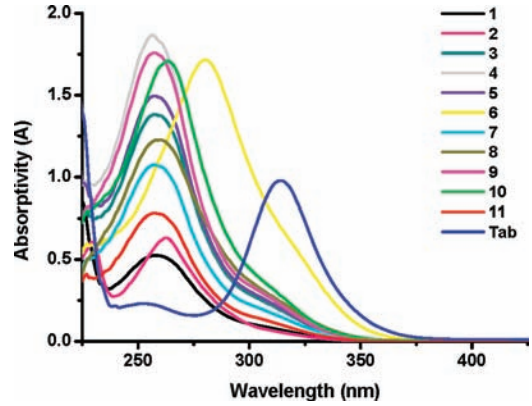

Figure 1. Electronic spectra of **1**−**11** and Tab in MeCN with a 1-mm optical length.

(Tab)-to-metal charge transfer.[14] Interestingly, when additional N-donor ligands are introduced into the $[Hg(Tab)_2]^{2+}$ linear framework of **1**, the main absorptions observed in the spectra of **2**−**5** and **7**−**11** are slightly red-shifted relative to that of **1**, which may reflect the slightly different coordination environments of the Hg atoms in these compounds. However, the absorption band of **6** remarkably deviates from those of **2**−**5** and **7**−**11**, suggesting that the Hg atom in **6** may hold a different coordination geometry. As observed in Hg^{II}-MerR/MT, $[Hg(SR)_2]$ (R = Et, ^{i}Pr),[7] mercury plastocyanin,[7d] and other MTs,[15] the low-energy UV transitions of 228−250 nm may be involved in the two- and three-coordination environments, while those in the range of 280−310 nm indicated a four-coordination geometry. In **2**−**11**, all of the main absorptions are in the range of 256−280 nm, suggesting that the coordination geometries around the Hg atoms in these complexes may not be the trigonally or tetrahedrally coordinated but in-between three- and four-coordinated, which is consistent with the observed results described later in this paper.

Crystal Structures of $[Hg(Tab)_2(L)](PF_6)_2\cdot S$ (2, L = phen, S = 2MeOH; 3, L = 2,2′-bipy, S = DMF), $[Hg(Tab)_2(L)_2](PF_6)_2$ (4, L = py; 5, L = N-Meim), and $[Hg(Tab)_2(N\text{-}^i Prim)](PF_6)_2$ (6). Compound **2** crystallizes in the monoclinic space group *C*2/*c*, while **3** crystallizes in the triclinic space group $P\bar{1}$. The asymmetric unit of **2** or **3** consists of a $[Hg(Tab)_2(L)]^{2+}$ dication, two PF_6^- anions, and two MeOH solvent molecules (**2**) or one DMF solvent molecule (**3**). Compound **4** crystallizes in the monoclinic space group *P*2/*c*, while **5** crystallizes in the triclinic space group $P\bar{1}$. The asymmetric unit of **4** or **5** contains a $[Hg(Tab)_2(L')_2]^{2+}$ dication and two PF_6^- anions. Compound **6** crystallizes in the orthorhombic space group *Fdd*2, and its asymmetric unit has one $[Hg(Tab)_2(N\text{-}^i Prim)]^{2+}$ dication and two PF_6^- anions. In the dication of **2** or **4**, there is an inversion center lying on the Hg atom and a crystallographic 2-fold axis running through the Hg atom. The central Hg atom in **2**−**5** is strongly coordinated by two S atoms of two Tab ligands and two N atoms from a phen (or 2,2′-bipy) ligand or two py or N-Meim ligands, forming a distorted

(9) (a) Chen, J. X.; Xu, Q. F.; Xu, Y.; Zhang, Y.; Chen, Z. N.; Lang, J. P. *Eur. J. Inorg. Chem.* **2004**, 4247. (b) Chen, J. X.; Xu, Q. F.; Zhang, Y.; Chen, Z. N.; Lang, J. P. *J. Organomet. Chem.* **2004**, *689*, 1071. (c) Chen, J. X.; Zhang, W. H.; Tang, X. Y.; Ren, Z. G.; Zhang, Y.; Lang, J. P. *Inorg. Chem.* **2006**, *45*, 2568. (d) Chen, J. X.; Zhang, W. H.; Tang, X. Y.; Ren, Z. G.; Li, H. X.; Zhang, Y.; Lang, J. P. *Inorg. Chem.* **2006**, *45*, 7671. (e) Ren, Z. G.; Tang, X. Y.; Li, L.; Liu, G. F.; Li, H. X.; Chen, Y.; Zhang, Y.; Lang, J. P. *Inorg. Chem. Commun.* **2007**, *10*, 1253. (f) Tang, X. Y.; Chen, J. X.; Liu, G. F.; Ren, Z. G.; Zhang, Y.; Lang, J. P. *Eur. J. Inorg. Chem.* **2008**, 2593. (g) Tang, X. Y.; Li, H. X.; Chen, J. X.; Ren, Z. G.; Lang, J. P. *Coord. Chem. Rev.* **2008**, *252*, 2026.

(10) (a) Bach, R. D.; Vardhan, H. B.; Maqsudur Rahman, A. F. M.; Oliver, J. P. *Organometallics* **1985**, *4*, 846. (b) Evans, C. A.; Rabenstein, D. L.; Geier, G.; Erni, I. W. *J. Am. Chem. Soc.* **1977**, *99*, 8106. (c) Sun, W. Y.; Zhang, L.; Yu, K. B. *J. Chem. Soc., Dalton Trans.* **1999**, 795. (d) Nockemann, P.; Schulz, F.; Naumann, D.; Meyer, G. *Z. Anorg. Allg. Chem.* **2005**, *631*, 649. (e) Zamora, F.; Kunsman, M.; Sabat, M.; Lippert, B. *Inorg. Chem.* **1997**, *36*, 1583. (f) Menzer, S.; Hillgeris, E. C.; Lippert, B. *Inorg. Chim. Acta* **1993**, *211*, 221. (g) Sheldrick, W. S.; Gross, P. *Inorg. Chim. Acta* **1989**, *156*, 139.

(11) (a) Chen, W. T.; Wang, M. S.; Cai, L. Z.; Guo, G. C.; Huang, J. S. *Aust. J. Chem.* **2005**, *58*, 578. (b) Duplancic, T.; Grdenic, D.; Kamenar, B.; Matkovic, P.; Sikirica, M. *J. Chem. Soc., Dalton Trans.* **1976**, 887. (c) Cannas, M.; Cristini, A.; Marongiu, G. *Inorg. Chim. Acta* **1976**, *18*, L10. (d) Jones, P. G. *Acta Crystallogr.* **1989**, *C45*, 173. (e) Tran, M. L.; Bernhardt, P. V.; Gentle, I. R. *Acta Crystallogr.* **2002**, *E58*, m150.

(12) (a) Gruenwedel, D. W.; Davidson, N. *J. Mol. Biol.* **1966**, *21*, 129. (b) Mulvihill, J. *Science* **1972**, *176*, 132.

(13) (a) Plappert, E. C.; Mingos, D. M. P.; Lawrence, S. E.; Willams, D. J. *J. Chem. Soc., Dalton Trans.* **1997**, 2119. (b) Kato, M.; Kojima, K.; Okamura, T.; Yamamoto, H.; Yamamura, T.; Ueyama, N. *Inorg. Chem.* **2005**, *44*, 4037.

(14) (a) Bharara, M. S.; Bui, T. H.; Parkin, S.; Atwood, D. A. *Inorg. Chem.* **2005**, *44*, 5753. (b) Bharara, M. S.; Parkin, S.; Atwood, D. A. *Inorg. Chem.* **2006**, *45*, 2112.

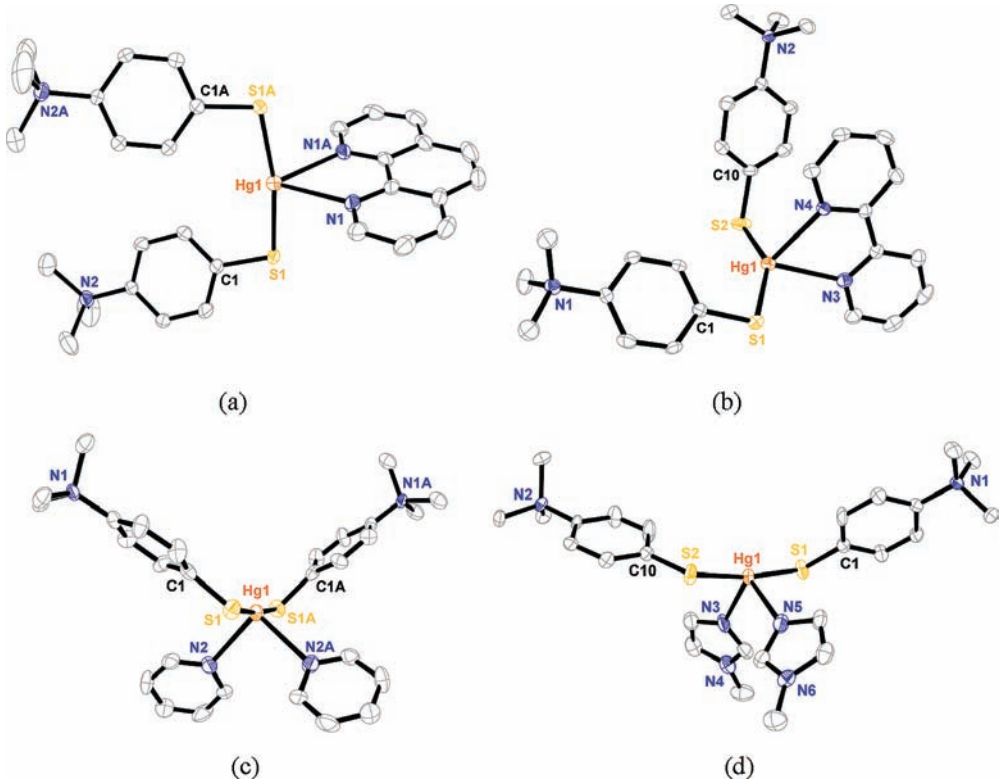

Figure 2. (a) Perspective view of the $[Hg(Tab)_2(phen)]^{2+}$ dication of **2**. Only one of the two orientations of the disordered Tab ligand is shown. Symmetry code: A, $1 - x$, y, $-z + {}^3/_2$. (b) Perspective view of the $[Hg(Tab)_2(2,2'\text{-bipy})]^{2+}$ dication of **3**. (c) Perspective view of the $[Hg(Tab)_2(py)_2]^{2+}$ dication of **4**. Only one of the two orientations of the disordered methyl groups is shown. Symmetry code: A, $-x$, y, ${}^1/_2 - z$. (d) Perspective view of $[Hg(Tab)_2(N\text{-}Meim)_2]^{2+}$ dication of **5**. The thermal ellipsoids were drawn at the 50% probability level. All H atoms have been omitted for clarity.

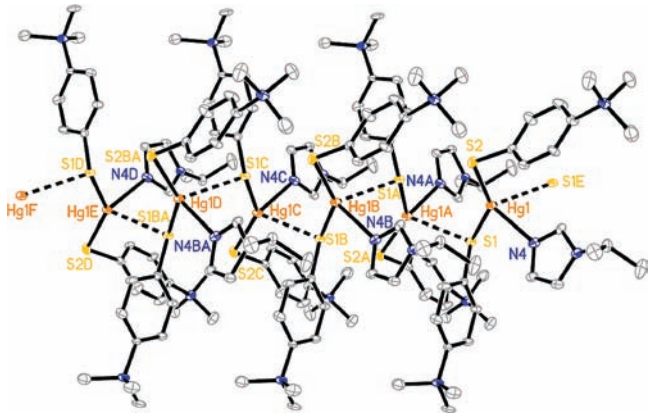

Figure 3. 1D chain (extending along the *c* axis) formed by weak Hg···S secondary interactions in **6**. The thermal ellipsoids were drawn at the 50% probability level. All H atoms have been omitted for clarity.

seesaw-shaped coordination geometry (Figure 2). Such a seesaw-shaped structure is observed in several mononuclear compounds such as $[Hg(Tab)_2(SCN)_2]$,[9c] $[Zn(neo)(SR)_2]$ ($R = CH_2CH_2C_6H_4$, p-$CH_3C_6H_4$; neo = neocuproine).[16a,b] In the dication of **6**, the central Hg1 atom is coordinated by two S atoms of the two Tab ligands and one N atom of the N-^{i}Prim ligand, forming a distorted T-shaped coordination geometry. These $[Hg(Tab)_2(N\text{-}^i Prim)]^{2+}$ dications are further connected with another S atom of the Tab ligand from the adjacent unit, affording a chain structure (Figure 3). To this end, the Hg center in **6** may be considered as having a pseudo-four-coordinated pinwheel-shaped geometry.

In the crystals of **2**−**3** and **5**−**6**, there are abundant intra- and intermolecular hydrogen-bonding interactions among the Tab ligands and counteranions and the crystal solvent molecules. For **2**, the S atoms of the Tab ligands interact with the H atoms of the methyl groups [C9···S1 (${}^3/_2 - x$, ${}^3/_2 - y$, $2 - z$)] and the phenyl groups [C5···S1 (${}^3/_2 - x$, ${}^3/_2 - y$, $2 - z$)] to afford intermolecular hydrogen bonds, forming a 1D chain structure (Figure S1 in the Supporting Information). For **3**, each pyridyl ring of 2,2′-bipy interacts with that of the nearest 2,2′-bipy via evident $\pi\cdots\pi$ interactions (3.662 Å), generating a chain structure (Figure 4). In addition, the PF_6^- anions in **3** are located in-between such 1D chains and interact with the H atoms of the phenyl and methyl groups of the Tab ligands, affording intramolecular hydrogen bonds [C17···F11 and C18···F8] and intermolecular hydrogen bonds [C16···F11 ($1 - x$, $1 - y$, $2 - z$)], forming a 2D hydrogen-bonded network along the [011] plane (Figure S2 in the Supporting Information). Furthermore, the O atoms of the solvated DMF molecules are involved in the hydrogen-bonding interactions with the H atoms of the phenyl groups of the Tab ligands [C3···O1 ($1 - x$, $1 - y$, $2 - z$)], methyl groups [C7···O1 ($1 - x$, $1 - y$, $2 - z$)], and the methyl groups from the nearby DMF molecules [C30···O1 ($2 - x$, $-y$, $2 - z$)], thereby generating a 3D hydrogen-bonded structure (Figure S3 in the Supporting Information).

For **5**, two intramolecular hydrogen-bonding interactions [C18···F5 and C18···F11] as well as six intermolecular hydrogen-bonding interactions between the F atoms and

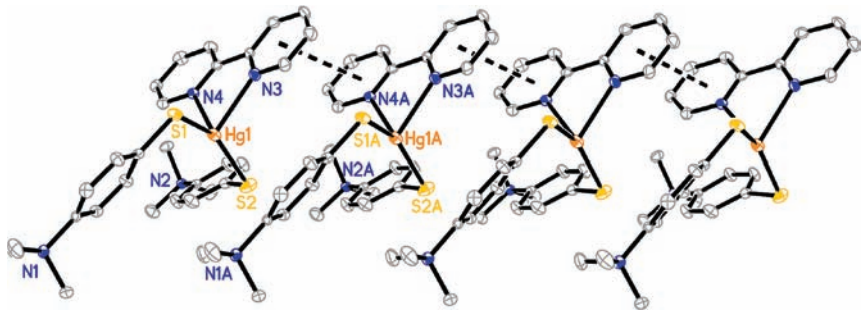

Figure 4. 1D chain extending along the *a* axis, formed by $\pi\cdots\pi$ interactions in **3**.

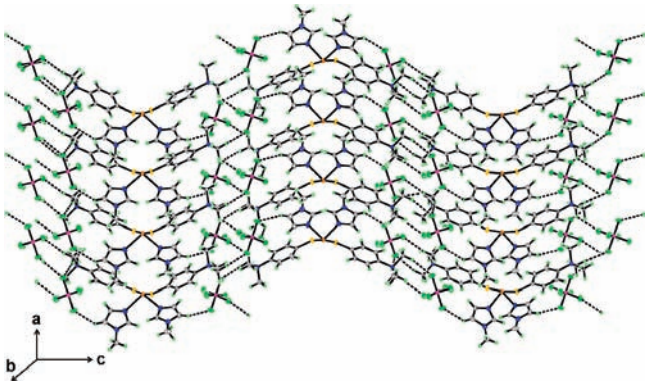

Figure 5. 2D wavelike structure extending along the *ac* plane formed by hydrogen-bonding interactions in **5**.

the H atoms of the methyl groups [C8···F2 (x, y, $1 + z$); C8···F6 ($1 - x$, $-y$, $1 - z$); C9···F6 (x, y, $1 + z$); C17···F12 ($-x$, $1 - y$, $-z$)] and the H atoms of the N-Meim ligands [C24···F1 ($1 - x$, $-y$, $1 - z$); C20···F9 ($1 + x$, y, z)] result in the formation of a 1D double chain running along the *c* axis. Each chain is held together by the intermolecular hydrogen-bonding interactions formed by the F10 atom and the H atom of the methyl group [C16···F10 ($1 - x$, $1 - y$, $-z$)], forming a 2D wavelike hydrogen-bonded network extending along the *ac* plane (Figure 5).

For **6**, the secondary Hg···S interactions [2.805(2) Å; Table 1] are much shorter than those in $[Hg(SCH_2COOH)_2]$ [3.379(3) Å][16c] and thus link the neighboring $[Hg(Tab)_2(N\text{-}^{i}Prim)]^{2+}$ dications into a 1D cationic chain extending along the *c* axis (Figure 3).

In addition, because the PF_6^- anions are located in-between these chains, several F atoms interact with the H atoms of the methyl groups [C8···F2 (x, y, $-1 + z$); C9···F6 (x, y, $-1 + z$); C17···F11 ($2 - x$, $^1/_2 - y$, $^1/_2 + z$)] and the H atoms of the phenyl groups [C12···F4 ($2 - x$, $^1/_2 - y$, $^1/_2 + z$)] of the Tab ligands and the H atoms of the imidazolyl rings [C22···F12 and C22···F10 ($^7/_4 - x$, $^1/_4 + y$, $-^1/_4 + z$)] and the H atoms of the methyl group [C16···F7 ($2 - x$, $^1/_2 - y$, $^1/_2 + z$)] of the N-^{i}Prim ligand to afford complicated intermolecular hydrogen bonds, forming a 3D hydrogen-bonded structure (Figure 6).

Crystal Structures of $[Hg(Tab)_2(L)](PF_6)_2\cdot 0.5MeCN$ (7, L = en; 8, L = eten) and $[Hg(Tab)_2(L)](PF_6)_2$ (9, L = tmen; 10, L = dap; 11, L = dpt). Compounds **7** and **8** crystallize in the monoclinic space group $C2/c$ (**7**) or $P2_1/n$ (**8**), and each asymmetric unit contains one independent $[Hg(Tab)_2(L)]^{2+}$ (L = en, eten) dication, two PF_6^- anions,

Table 1. Selected Bond Distances (Å) and Angles (deg) for **2**−**11**

Compound **2**			
Hg1−S1	2.344(3)	Hg1−N1	2.540(5)
S1−Hg1−S1A	169.28(14)	N1−Hg1−N1A	65.4(2)
S1−Hg1−N1	89.22(14)	S1−Hg1−N1A	99.84(14)
Compound **3**			
Hg1−S1	2.3768(14)	Hg1−S2	2.3921(14)
Hg1−N3	2.469(3)	Hg1−N4	2.490(3)
S1−Hg1−S2	148.27(4)	N3−Hg−N4	66.52(11)
S1−Hg1−N3	99.08(9)	S1−Hg1−N4	108.22(8)
S2−Hg1−N4	99.76(8)	S2−Hg1−N3	105.69(9)
Compound **4**			
Hg1−S1	2.345(3)	Hg1−N2	2.651(9)
S1−Hg1−S1A	173.72(13)	N2−Hg1−N2A	98.3(4)
S1A−Hg1−N2	80.9(2)	S1−Hg1−N2	103.3(2)
Compound **5**			
Hg1−S1	2.3718(16)	Hg1−S2	2.3678(16)
Hg1−N3	2.553(5)	Hg1−N5	2.559(5)
S1−Hg1−S2	171.92(6)	N3−Hg1−N5	107.39(17)
S1−Hg1−N3	82.06(12)	S2−Hg1−N5	81.34(12)
S1−Hg1−N5	102.68(12)	S2−Hg1−N3	103.57(12)
Compound **6**			
Hg1−S1	2.435(2)	Hg1−S2	2.389(2)
Hg1−S1A	2.805(2)	Hg1−N4	2.440(8)
S1−Hg1−S2	142.29(8)	S2−Hg1−N4	107.20(18)
S1−Hg1−N4	102.82(17)	S2−Hg1−S1A	107.53(8)
S1−Hg1−S1A	100.09(6)	N4−Hg1−S1A	79.0(2)
Compound **7**			
Hg1−S1	2.440(17)	Hg1−S2	2.409(13)
Hg1−N3	2.48(3)	Hg1−N4	2.43(2)
S1−Hg1−S2	140.6(5)	N3−Hg1−N4	71.6(7)
S1−Hg1−N3	103.1(7)	S2−Hg1−N4	98.9(7)
S1−Hg1−N4	115.9(7)	S2−Hg1−N3	105.0(7)
Compound **8**			
Hg1−S1	2.385(5)	Hg1−S2	2.392(5)
Hg1−N3	2.436(17)	Hg1−N4	2.463(14)
S1−Hg1−S2	144.23(18)	N3−Hg1−N4	73.8(6)
S1−Hg1−N3	102.8(4)	S2−Hg1−N4	110.7(4)
S1−Hg1−N4	98.6(4)	S2−Hg1−N3	104.6(4)
Compound **9**			
Hg1−S1	2.3885(19)	Hg1−S2	2.3953(19)
Hg1−N3	2.503(7)	Hg1−N4	2.508(6)
S1−Hg1−S2	151.84(8)	N3−Hg1−N4	74.4(3)
S1−Hg1−N3	93.55(17)	S2−Hg1−N4	93.19(16)
S1−Hg1−N4	111.32(16)	S2−Hg1−N3	106.70(17)
Compound **10**			
Hg1−S1	2.4028(19)	Hg1−S2	2.413(2)
Hg1−N3	2.466(6)	Hg1−N4	2.475(5)
S1−Hg1−S2	147.09(7)	N3−Hg1−N4	78.2(2)
S1−Hg1−N3	103.78(18)	S2−Hg1−N4	110.64(13)
S1−Hg1−N4	95.43(14)	S2−Hg1−N3	101.00(17)
Compound **11**			
Hg1−S1	2.3892(14)	Hg1−S2	2.4018(15)
Hg1−N3	2.411(2)	Hg1−N4	2.533(2)
S1−Hg1−S2	150.66(5)	N3−Hg1−N4	78.56(7)
S1−Hg1−N3	105.00(7)	S2−Hg1−N4	94.57(6)
S1−Hg1−N4	108.78(6)	S2−Hg1−N3	96.67(7)

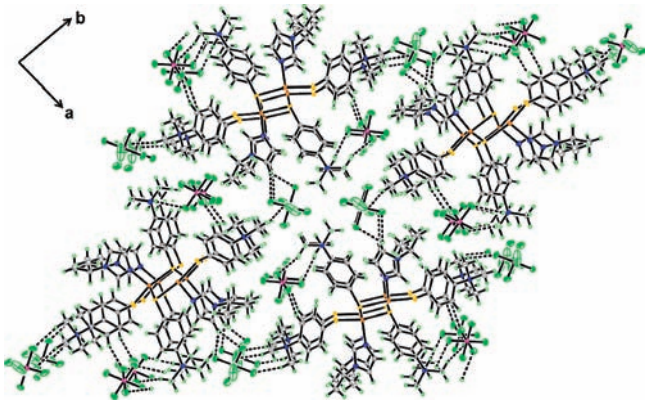

Figure 6. 3D structure formed by Hg···S secondary interactions and intermolecular hydrogen-bonding interactions in **6** (looking along the *c* axis).

and half of a MeCN solvent molecule. Compounds **9**−**11** crystallize in the triclinic space group $P\bar{1}$, and the asymmetric unit consists of one discrete $[Hg(Tab)_2(L)]^{2+}$ (L = tmen, dap, dpt) dication and two PF_6^- anions. Because the structure of the dication of **8** is quite similar to that of **7**, only the perspective view of the dication of **7** along with the structures of the dications of **9**−**11** are shown in Figure 7. In each $[Hg(Tab)_2(L)]^{2+}$ cation, the Hg center is coordinated by two S atoms from Tab ligands and chelated by two N atoms from one diamine ligand (en for **7**, eten for **8**, tmen for **9**, or dap for **10**) or one triamine ligand dpt (**11**), displaying a distorted seesaw-shaped coordination geometry.

The hydrogen-bonding interactions in **7**−**8** and **10**−**11** are also rich and complicated. For **7**, intermolecular hydrogen-bonding interactions between the H atoms of the NH_2 groups from en and the S atoms of Tab [N3···S1 ($-x$, $1 - y$, $1 - z$); N4···S2 ($-x$, y, $^3/_2 - z$)] and the F atoms of the PF_6^- anions [N4···F8 ($-1 + x$, $2 - y$, $^1/_2 + z$)] and between the H atoms of the methyl groups from Tab and the F atoms from the PF_6^- anion [C5···F11 ($-1 + x$, $2 - y$, $^1/_2 + z$)] afford a 1D chain running along the *c* axis (Figure S4 in the Supporting Information). Each chain is linked with the neighboring ones by hydrogen-bonding interactions [C7···F1 ($-1 + x$, y, z); C9···F10 ($-1 + x$, y, z)], forming a 2D layer extending along the *bc* plane. Furthermore, adjacent layers are connected by hydrogen-bonding interactions [C17···F12 ($-^1/_2 + x$, $-^1/_2 + y$, $1 + z$); C18···F9 ($-^1/_2 + x$, $-^1/_2 + y$, $1 + z$)] into a 3D hydrogen-bonded structure (Figure 8).

For **8**, there exist several intermolecular hydrogen-bonding interactions between the H atoms of the NH_2 groups of eten and the S atoms of Tab [N3···S2 ($^3/_2 - x$, $^1/_2 + y$, $^1/_2 - z$)] and between the H atoms of the MeCN solvent molecule and the F atoms of the PF_6^- anions [C24···S2 ($-1 + x$, $-y$, $-z$)], which lead to the formation of a 1D chain extending along the *b* axis (Figure 9).

For **10**, the S atoms of the Tab ligands are engaged in intermolecular hydrogen-bonding interaction with the H atoms of the phenyl groups of the adjacent Tab ligands [C12···S1 ($2 - x$, $-y$, $2 - z$)], forming a 14-membered ring. Such rings are connected to each other by interactions between the F atoms of the PF_6^- anions and the H atoms of the phenyl groups [C3···F10 ($1 - x$, $-y$, $1 - z$)], the methyl groups [C9···F10 ($1 - x$, $-y$, $1 - z$); C8···F7 ($1 - x$, $-y$, $1 - z$)], and the amino groups [N4···F10 (x, y, $1 + z$)], generating a 1D hydrogen-bonded chain running along the *a* axis (Figure S5 in the Supporting Information). Each chain is held together into a 2D hydrogen-bonded network (extending along the *ab* plane) by intermolecular hydrogen-bonding interactions between the F atoms of the PF_6^- anions and the H atoms of the amino groups [N4···F12 ($2 - x$, $1 - y$, $2 - z$)] and the methyl groups [C7···F3 ($1 - x$, $-y$, $1 - z$); C17···F4 ($2 - x$, $1 - y$, $2 - z$)] (Figure 10).

In the case of **11**, there are several intermolecular hydrogen-bonding interactions between the H atoms of the amino groups of the dpt ligands and the S atoms of the Tab ligands [N3···S2 ($1 - x$, $1 - y$, $1 - z$)] and the N atoms of the amino groups [N3···N5 ($1 - x$, $2 - y$, $1 - z$)] from the neighboring $[Hg(Tab)_2(dpt)]^{2+}$ dications, thereby forming a 1D chain running along the *b* axis (Figure 11).

Variations in the Configurations of $Hg(Tab)_2$ Units of 2−11. Previously, halide and halide/N binding to mercury(II) dithiolates were reported to result in structure changes including bending of the S−Hg−S bonds.[14a,b] The Hg−X (X = Cl, Br, I) interactions tended to linking the Hg/S species into polymeric structures, while the Hg−N interactions formed discrete complexes. In our cases, upon coordination of the N-donor ligands onto the Hg center of the $[Hg(Tab)_2]^{2+}$ dication of **1**, its original configuration of $Hg(Tab)_2$ units was also changed. Therefore, these variations in the configurations of $Hg(Tab)_2$ units in **2**−**11** deserve comment. When closely looking into the structures of **2**−**11**, the original trans configuration of the $Hg(Tab)_2$ unit of **1** is remarkably affected by coordination of the N-donor ligands at the Hg center. Three configuration variations were observed in these compounds (Scheme 3). The first one is the rotation of the two Tab groups around the S−Hg−S line. Relieving the large steric crowding among the Tab groups and the introduced N-donor ligands in **2**−**11** may be its impetus. Such a rotation can result in bending of the S−Hg−S bond and the changes in the Hg−S bond lengths and the S−Hg−S bond angles (Table 2). For example, one of the two Tab groups in **2** turns by ca. 180° around the S1−Hg1−S1A line, which makes the two Tab ligands oriented in the same direction with a dihedral angle of 14.16° between one plane composed of N1, S1, and Hg1 atoms and the other of N1A, S1A, and Hg1 atoms. For **3**, **4**, or **6**, the two Tab ligands rotate by ca. 90° around the S−Hg−S line and are in the approximately mutually perpendicular position with a dihedral angle between the similar planes, being 86.48° (**3**), 82.46° (**4**), or 85.74° (**6**). In the case of **5**, both Tab ligands turn by ca. 40° around the S1−Hg1−S2 contact and nearly directly in opposite orientations with a dihedral angle of 50.89°. However, the trans configuration of the two Tab groups of **1** is almost retained in each $[Hg(Tab)_2(L)]^{2+}$ (L = en, eten) dication of **7** or **8**. Only a slight rotation of both groups along the S−Hg−S line is observed because their dihedral angles are 4.87° and 5.87°, respectively. For **9**, both groups are almost perpendicular to each other, with the dihedral angle being 67.26°, while those in **10** or **11** are

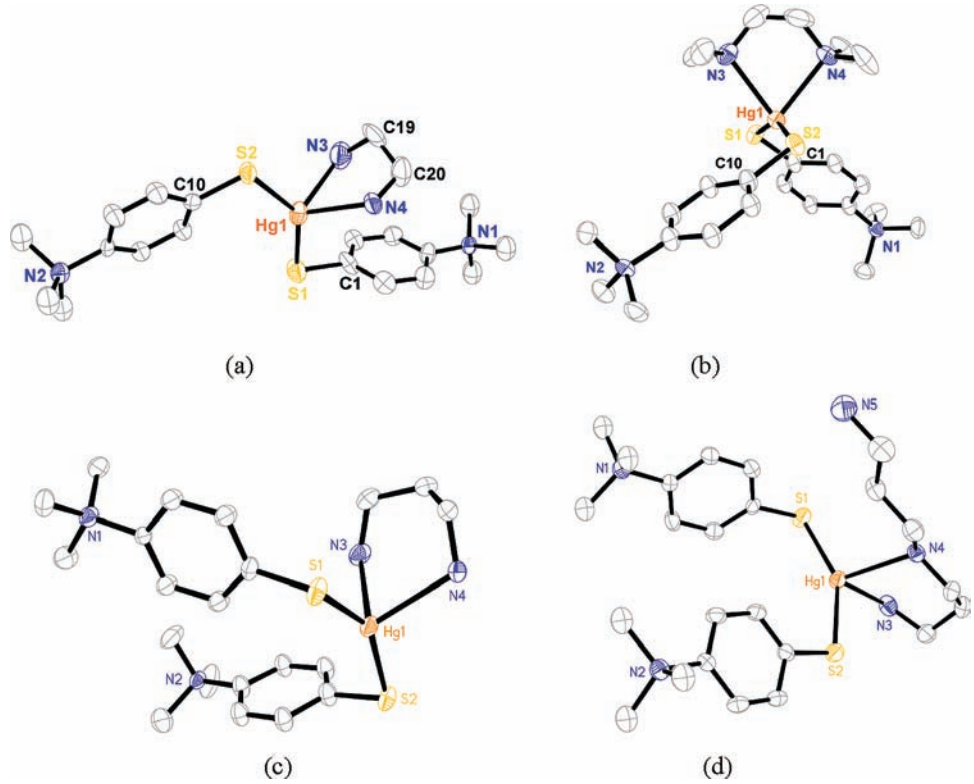

Figure 7. (a) Perspective view of the $[Hg(Tab)_2(en)]^{2+}$ dication in **7**. (b) Perspective view of the $[Hg(Tab)_2(tmen)]^{2+}$ dication in **9**. (c) Perspective view of the $[Hg(Tab)_2(dap)]^{2+}$ dication in **10**. (d) Perspective view of the $[Hg(Tab)_2(dpt)]^{2+}$ dication in **11**. Only one of the two orientations of the disordered Tab ligand is shown. The thermal ellipsoids were drawn at the 50% probability level. All H atoms are omitted for clarity.

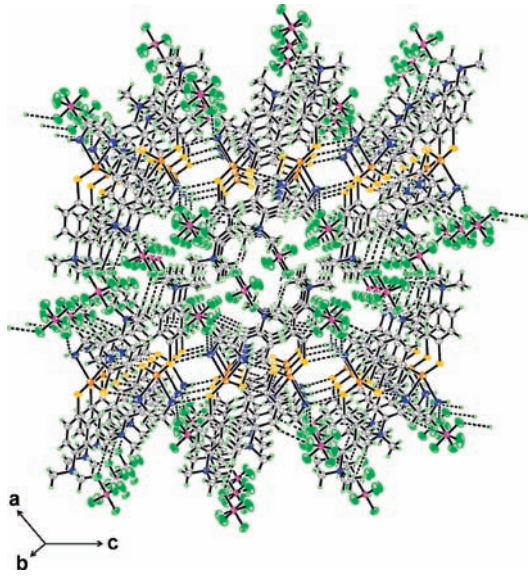

Figure 8. 3D structure formed by intermolecular hydrogen-bonding interactions in **7** (looking along the *b* axis). All H atoms except those involved in hydrogen-bonding interactions were omitted.

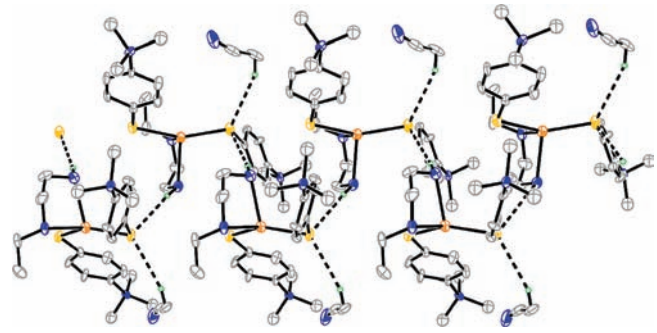

Figure 9. 1D chain along the *b* axis formed by hydrogen-bonding interactions in **8**. All H atoms except those related to hydrogen-bonding interactions were omitted.

almost in the same direction, with the dihedral angle being 33.86° (**10**) or 15.30° (**11**).

The second one is the swing of the two Tab groups along the S−Hg−S line. Such a swing resulted in deviation of the two N(Tab)−S−Hg angles in **2**−**11** from those of the corresponding ones in **1** (Table 2). When the N-donor ligands and the two Tab groups lie in the same plane, the large steric hindrance among them understandably enlarges the N(Tab)−S−Hg angle and both Tab groups thus swing outward. The largest deviation for one N(Tab)−S−Hg angle was observed in **11** (11.20°). However, when both Tab groups and the N-donor ligands are staggered and not in the same plane, the steric hindrance between is relieved and both Tab groups swing inward. In the cases of **7**, **8**, **10**, several N(Tab)−S−Hg angles get contracted relative to those of **1** and the largest contract (8.48°) is found in **10**.

The third one is the rotation of the two phenyl groups of the Tab ligands in **2**−**11**. As described previously, the two phenyl groups of **1** are in a parallel position. Both groups in **2**−**11** were found to rotate by some degrees along the S−N(Tab) line to deviate from their original parallel position. The dihedral angles between the phenyl groups of the Tab ligands in **2**−**11** are 20.62° (**2**), 30.48° (**3**), 74.88° (**4**), 74.92° (**5**), 77.28° (**6**), 70.39° (**7**), 79.10° (**8**), 72.59° (**9**), 87.47° (**10**), and 61.18° (**11**), respectively.

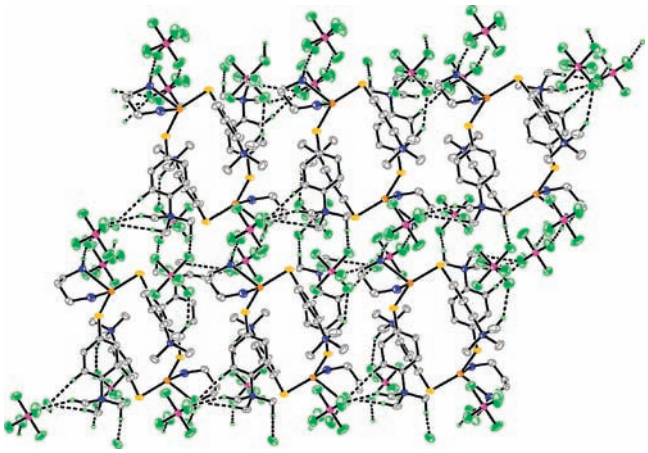

Figure 10. 2D network along the *ab* plane formed via hydrogen-bonding interactions in **10**. All H atoms except those engaged in hydrogen-bonding interactions were omitted.

Because of the existence of the three configuration variations, the Hg−S bond lengths of **2**−**11** are correspondingly changed. As shown in Table 3, the mean Hg−S distance of **2** is longer than that in $[Hg(SCH_2CH_2CH_2Et)_2]$[17a] but somewhat shorter than those in **3**, **5**, and $[Hg(SCH_2CH_2NH_2)_2]$ [2.361(3) Å][1a] and remarkably shorter than those in **6**−**11**. It is in good agreement with those of **1**,[9c] **4**, $[HgR_2]$ (R = SEt,[17b] 2-Spy,[17c] SMe,[17d] HCys/H_2Cys[17e]), and $\{[Hg(\mu\text{-}SC_6H_4OCH_3\text{-}p)(2,2'\text{-bipy})](PF_6)\}_n$ [2.348(2) Å].[18] Among all of these complexes, the Hg−S bond length [2.425(13) Å] of **7** is the longest. It is noted that the mean Hg−S bond lengths of **2**−**5** and **7**−**11** do not match those of four-coordinated mercury(II) thiolate complexes such as $[Hg(4\text{-}SpyH)_2(4\text{-}Spy)_2]$ [2.520(2)−2.577(3) Å, 4-Spy = pyridine-4-thiolate] and $[HgL_4]^-$ [2.527(2)−2.552(2) Å for L = 4-chlorobenzenethiolate; 2.520(3) Å for L = 2-phenylbenzenethiolate; 2.551(3) Å for L = 2-(*N*-methylcarbamoyl)phenylthiolate][6f,g,13b,19] but are close to the EXAFS data for the three-coordinated Hg centers in Hg-MerR,[6c,20] Hg_7-MT,[21] and Hg_{18}-MT.[22] We assumed that the bond lengths in the range of 2.344−2.425 Å are special for the seesaw-shaped four-coordinated $[HgS_2N_2]$. On the other hand, the average Hg−N bond length of **4** is longer than those in **2**, **3**, **5**, **6**, and $[Hg(SCH_2CH_2NH_2)_2]$ [2.361(4) Å][1a] and $[Hg(btzt)_2(2,2'\text{-bipy})]$ [2.457(2) Å; btzt = 1,3-benzothiazole-2-thione][8a] but shorter than that in $[Hg(S\text{-}2\text{-}N_2C_4H_3)_2]$ [2.880(3) Å; S-2-$N_2C_4H_3$ = pyrimidine-2-thiolato].[23] The average Hg−N lengths in **7**−**11** are in the range of 2.46(2)−2.506(6) Å, which are somewhat shorter than those of **2**−**5**.

Variations in the configuration of the $Hg(Tab)_2$ unit also result in changes of the S−Hg−S angles. The S−Hg−S bond angles in **2**, **4**, and **5** are 169.28°, 173.72°, and 171.92°, which almost retain the linear S−Hg−S angle of **1**. However, the S−Hg−S bond angle in **3** is 148.27°. As discussed early in this paper, one Tab group in **2** rotates by ca. 180° around the S−Hg−S line, while that in **3** rotates by ca. 90°. Evidently, the former holds smaller steric hindrance among phen and Tab groups than the latter, which may account for the fact that the deviation in **2** (10.72°) is smaller than that in **3** (31.73°). For **6**, the S−Hg−S angle is 142.29°, which is understandable for a three-coordinated T-shaped Hg center. The S−Hg−S bond angles in **7**−**11** vary from 140.6° to 151.84°, which greatly deviates from that of **1**. The values of **9**−**11** are comparable to that of **3** but larger than those of **7** and **8**. The rotation and swinging of the two Tab groups in these complexes decide on the steric crowding among them and the N-donor ligands, which is responsive to their deviation from the linear S−Hg−S angle of **1**. In addition, the N−Hg−N bite angle of **3** is close to those in **2** and $[Hg(S\text{-}2\text{-}N_2C_4H_3)_2]$ [66.9(1)°][8a] but somewhat smaller than that in $\{[Hg(\mu\text{-}SC_6H_4OCH_3\text{-}p)(2,2'\text{-bipy})](PF_6)\}_n$ [73.2(2)°].[18] Because of the rigidness of the phen or 2,2′-bipy ligand in **2** or **3**, their N−Hg−N bite angles are remarkably smaller than those of **4** and **5**. The N−Hg−N bite angles in **7**−**9** are larger than those of **2** and **3** but smaller than those of **10** and **11**. The former difference may be due to the formation of a less rigid five-membered ring in **7**−**9**, while the latter may be ascribed to the formation of a more flexible six-membered ring in **10** and **11**.

Concluding Remarks

We have demonstrated the interesting reactivity of a precursor complex **1** towards heterocyclic ligands (phen, 2,2′-bipy, phen, py, N-Meim, and N-^{i}Prim) and alkyldiamine or triamine ligands (en, eten, tmen, dap, and dpt) and the successful isolation of 10 new Hg/Tab/L (L = N-donor ligand) adduct complexes (**2**−**11**). According to their X-ray analysis, the linear coordination geometry of the Hg^{II} center in **1** is converted into pseudo-pinwheel-shaped four-coordinated (**6**) and seesaw-shaped four-coordinated (**2**−**5** and **7**−**11**) fashions in **2**−**11** when the Hg center is coordinated by these N-donor ligands. More importantly, the trans configuration of the dication of **1** is found to undergo changes in **2**−**11** in three ways: the rotation of the two Tab groups around the S−Hg−S line, the swing of the two Tab groups along the S−Hg−S line, and the rotation of the two phenyl groups of the Tab ligands along the S−N(Tab) line. These configuration variations result in changes of the Hg−S

(15) Beltramine, M.; Lerch, K.; Vasak, M. *Biochemistry* **1984**, *23*, 3422.
(16) (a) Seebacher, J.; Ji, M.; Vahrenkamp, H. *Eur. J. Inorg. Chem.* **2004**, 409. (b) Burth, R.; Vahrenkamp, H. *Inorg. Chim. Acta* **1998**, *282*, 193. (c) Bramlett, J. M.; Im, H. J.; Yu, X. H.; Chen, T.; Cai, H.; Roecker, L. E.; Barnes, C. E.; Dai, S.; Xue, Z. L. *Inorg. Chim. Acta* **2004**, *357*, 243.
(17) (a) Hoffmann, G. G.; Steinfatt, I.; Brockner, W.; Kaiser, V. *Z. Naturforsch.* **1999**, *54b*, 887. (b) Fraser, K. A.; Clegg, W.; Craig, D. C.; Scudder, M. L.; Dance, I. G. *Acta Crystallogr.* **1995**, *C51*, 406. (c) Wang, S. N.; Fackler, J. P., Jr. *Inorg. Chem.* **1989**, *28*, 2615. (d) Bradley, D. C.; Kunchur, N. R. *J. Chem. Phys.* **1964**, *40*, 2258. (e) Taylor, N. J.; Carty, A. J. *J. Am. Chem. Soc.* **1977**, *99*, 6143.
(18) Yam, V. W. W.; Pui, Y. L.; Cheung, K. K. *J. Chem. Soc., Dalton Trans.* **2000**, 3658.
(19) (a) Anjali, K. S.; Vittal, J. J.; Dean, P. A. W. *Inorg. Chim. Acta* **2003**, *79*, 351. (b) Manceau, A.; Nagy, K. L. *J. Chem. Soc., Dalton Trans.* **2008**, 1421.
(20) Jaliehvand, F.; Leung, B. O.; Izadifard, M.; Damian, E. *Inorg. Chem.* **2006**, *45*, 66.
(21) Hasnain, S. S. In *Synchrotron Radiation in Chemistry and Biology II*; Mandelkow, E., Ed.; Springer-Verlag: New York, 1988; p 73.
(22) (a) Jiang, D. T.; Heald, S. M.; Sham, T. K.; Stillman, M. J. *J. Am. Chem. Soc.* **1994**, *116*, 11004. (b) Lu, W. H.; Kasrai, M.; Bancroft, G. M.; Stillman, M. J.; Tan, K. H. *Inorg. Chem.* **1990**, *29*, 2561.
(23) Eichhofer, A.; Buth, G. *Eur. J. Inorg. Chem.* **2005**, 4160.

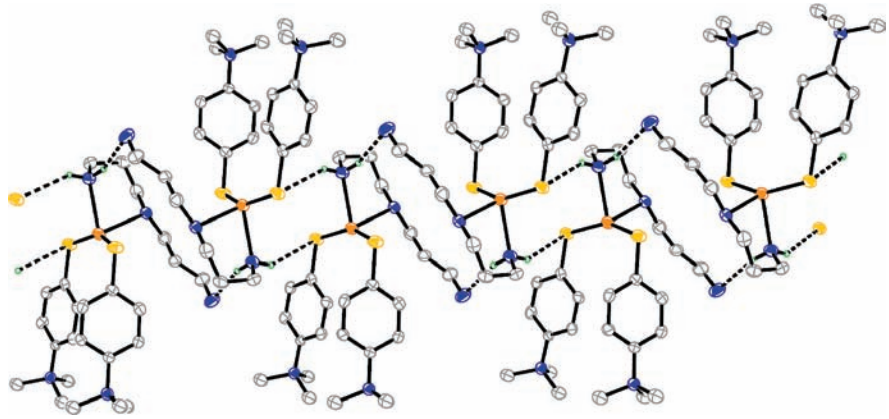

Figure 11. 1D chain running along the *b* axis formed by hydrogen-bonding interactions in **11**. All H atoms except those involved in hydrogen-bonding interactions were omitted.

Scheme 3. Conversions from the Trans Configuration of the $Hg(Tab)_2$ Unit of **1** to Other Configurations of the $Hg(Tab)_2$ Units of **2**−**11**

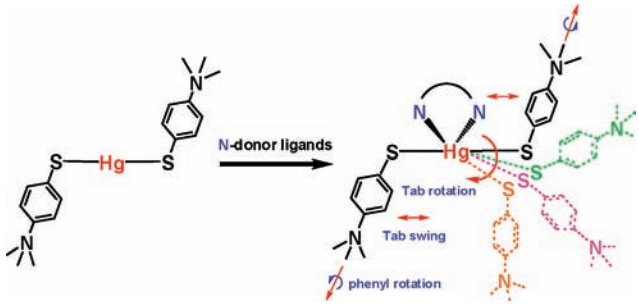

bond lengths and the S−Hg−S bond angles in **2**−**11**. Because the bond lengths of 2.344−2.425 Å in **2**−**11** do not fall into those of complexes containing tetrahedrally coordinated Hg, they may be established for the seesaw-shaped four-coordinated $[HgS_2N_2]$. The results suggested that the geometry of the Hg sites of Hg-MerR and Hg-MT might be changed when they are attacked by N-donor ligands either from these proteins or from the surrounding species like amines, N-heterocyclic compounds, and other biobases. They may also be useful in the interpretion of the structural data of Hg-MerR and Hg-MT from EXAFS, NMR, UV−vis, and Raman spectroscopic studies. We are currently extending this work by investigating the reactivity of **1** toward naturally encountered alkylcarboxylic acids (acetate acid, propionic acid, malonic acid, etc.) or aromatic carboxylic acids (benzoic acid, salicylic acid, nicotinic acid, etc.).

Experimental Section

General Procedures. Complex **1** was prepared according to the literature method.[9c] Other chemicals and reagents were used as purchased. All solvents were predried over activated molecular sieves and refluxed over appropriate drying agents under argon. IR spectra were recorded on a Varian 1000 FT-IR spectrometer as KBr disks (4000−400 cm^{-1}). UV−vis spectra were measured on a Varian 50 UV−visible spectrophotometer. Elemental analyses for C, H, and N were performed on a Carlo-Erba CHNO-S microanalyzer. ^1H NMR spectra were recorded at ambient temperature on a Varian UNITYplus-400 spectrometer. ^1H NMR chemical shifts were referenced to the deuterated dimethyl sulfoxide $[(CD_3)_2SO]$ signal.

$[Hg(Tab)_2(phen)](PF_6)_2\cdot 2MeOH$ (2). To a solution of **1** (0.825 g, 1 mmol) in DMF (1 mL) and MeCN (5 mL) was added a solution of phen (0.360 g, 2 mmol) in MeOH (8 mL). The mixture was briefly stirred and filtered. Slow evaporation of the solvents from the colorless filtrate afforded colorless blocks of **2**. Yield: 0.92 g (86% based on Hg). Anal. Calcd for $C_{32}H_{42}HgN_4O_2S_2F_{12}P_2$: C, 35.94; H, 3.96; N, 5.24. Found: C, 35.68; H, 3.72; N, 5.33. IR (KBr disk): 1667 (s), 1582 (w), 1490 (s), 1420 (m), 1389 (m), 1127 (w), 1096 (w), 1011 (w), 957 (w), 841(s), 726 (w), 556 (s) cm^{-1}. UV−vis [MeCN; λ_{max}, nm (ϵ, M^{-1} cm^{-1})]: 263 (126 500). ^1H NMR [400 MHz, $(CD_3)_2SO$]: δ 9.08 (d, 2H, phen), 8.60 (d, 2H, phen), 8.04 (br s, 2H, phen), 7.34−7.45 (m, 8H, Ph), δ 7.90 (t, 2H, phen), 3.42 (s, 18H, NMe_3).

$[Hg(Tab)_2(2,2'\text{-bipy})](PF_6)_2\cdot DMF$ (3). Compound **3** was prepared as colorless prism crystals in a manner similar to that described for the preparation of **2**, using 2,2-bipy (0.312 g, 2 mmol) as a starting material. Yield: 0.96 g (91% based on Hg). Anal. Calcd for $C_{31}H_{41}HgF_{12}N_5OP_2S_2$: C, 35.31; H, 3.92; N, 6.64. Found: C, 35.42; H, 3.67; N, 6.48. IR (KBr disk): 1670 (s), 1591 (w), 1489 (s), 1438 (m), 1315(w), 1126 (m), 1010 (w), 960 (w), 836 (s), 762 (m), 558 (s) cm^{-1}. UV−vis [MeCN; λ_{max}, nm (ϵ, M^{-1} cm^{-1})]: 258 (138 400). ^1H NMR [400 MHz, $(CD_3)_2SO$]: δ 8.69 (d, 2H, 2,2′-bipy), 8.39 (d, 2H, 2,2′-bipy), 7.95 (t, 2H, 2,2′-bipy), 7.59−7.72 (m, 8H, Ph), 7.45 (t, 2H, 2,2′-bipy), 3.55 (s, 18H, NMe_3).

$[Hg(Tab)_2(py)_2](PF_6)_2$ (4). To a solution containing **1** (0.825 g, 1 mmol) in MeCN (15 mL) was added pyridine (1 mL). The resulting mixture was stirred for 4 h, forming a homogeneous solution. After filtration, diethyl ether (40 mL) was allowed to diffuse into the filtrate at ambient temperature for 1 week, forming colorless plates of **4**, which were collected by filtration, washed with Et_2O, and dried in vacuo. Yield: 0.86 g (87% based on Hg). Anal. Calcd for $C_{28}H_{36}F_{12}HgN_4P_2S_2$: C, 34.20; H, 3.69; N, 5.70. Found: C, 34.12; H, 3.50; N, 5.86. IR (KBr disk): 1590 (m), 1490 (s), 1443 (m), 1412 (w), 1127 (w), 1011 (w), 957 (m), 841 (s), 749 (w), 702 (m), 556 (s) cm^{-1}. UV−vis [MeCN; λ_{max}, nm (ϵ, M^{-1} cm^{-1})]: 256 (93 300). ^1H NMR [400 MHz, $(CD_3)_2SO$]: δ 8.58 (d, 4H, py), 7.76−7.80 (m, 2H, py), 7.60−7.74 (m, 8H, Ph), 7.36−7.39 (m, 4H, py), 3.55 (s, 18H, NMe_3).

$[Hg(Tab)_2(N\text{-}Meim)_2](PF_6)_2$ (5). Compound **5** was prepared as colorless needles in a manner similar to that described for the preparation of **4**, using N-Meim (0.165 g, 2 mmol) as a starting material. Yield: 0.91 g (92% based on Hg). Anal. Calcd for $C_{26}H_{38}HgN_6P_2F_{12}S_2$: C, 31.57; H, 3.87; N, 8.50. Found: C, 31.29; H, 3.59; N, 8.61. IR (KBr disk): 1648 (w), 1586 (w), 1489 (s), 1414 (m), 1284 (w), 1231 (m), 1128 (m), 1108 (m), 1083 (m), 1011 (m), 958 (m), 923 (m), 838 (s), 759 (m), 660 (m), 558 (s) cm^{-1}. UV−vis [MeCN; λ_{max}, nm (ϵ, M^{-1} cm^{-1})]: 257 (149 900). ^1H NMR [400 MHz, $(CD_3)_2SO$]: δ 7.59−7.73 (m, 8H, Ph), 7.55

Table 2. S−Hg−S, N(Tab)−S−Hg, and N−Hg−N Bond Angles (deg) and Hg−S Bond Lengths (Å) in **1**−**11**

	1[9c]	**2**	**3**	**4**	**5**	**6**	**7**	**8**	**9**	**10**	**11**
S−Hg−S	180	169.28	148.27	173.72	171.92	142.29	140.6	144.23	151.84	147.09	150.66
Hg−S	2.331	2.344	2.3768	2.345	2.3718	2.435	2.440	2.385	2.3885	2.4028	2.3892
Hg−S	2.331	2.344	2.3921	2.345	2.3678	2.389	2.409	2.392	2.3953	2.413	2.4018
N(Tab)−S−Hg	104.16	107.28	106.75	114.60	113.89	110.34	108.07	102.38	107.98	95.68	115.36
N(Tab)−S−Hg	104.16	105.97	106.75	114.60	112.81	109.06	97.10	111.14	110.32	111.58	105.68
N−Hg−N		65.4	66.52	98.3	107.39		71.6	73.8	74.4	78.2	78.56

Table 3. Hg−S Bond Lengths (Å) in **1**−**11** and Other Mercury(II) Thiolate Compounds

compound	Hg−S	ref
$[Hg(SCH_2CH_2CH_2Et)_2]$	2.304	17a
$[Hg(SEt)_2]$	2.343	17b
$[Hg(2\text{-}Spy)_2]$	2.356	17c
$[Hg(SMe)_2]$	2.360	17d
$[Hg(HCys)(H_2Cys)]Cl\cdot 0.5H_2O$	2.329−2.355	17e
$[Hg(4\text{-}SpyH)_2(4\text{-}Spy)_2]$[a]	2.520(2)−2.577(3)	19
Hg-MerR	2.42−2.43	6c, 20
Hg_7-MT	2.33−2.42	21
Hg_{18}-MT	2.41−2.42	22
$[Hg(Cys)_2]^{2-}$	2.32−2.36	21
$[Hg(Cys)_3]^{4-}$	2.43−2.45	22
$[Et_4N][Hg(S^tBu)_3]$	2.436−2.451	7
$[n\text{-}Pr_4N][Hg(S\text{-}2,4,5\text{-}{}^i Pr_3C_6H_2)_3]$	2.397−2.469	4c
$[HgL_4]^-$	2.527(2)−2.552(2)[b]	6g
	2.520(3)[c]	6f
	2.551(3)[d]	13b
1	2.331(2)	9c
2	2.344(3)	this work
3	2.3845(14)	this work
4	2.345(3)	this work
5	2.3698(16)	this work
6	2.412(2)	this work
7	2.425	this work
8	2.389(5)	this work
9	2.3919(19)	this work
10	2.408	this work
11	2.3956	this work

[a] 4-Spy = pyridine-4-thiolate. [b] L = 4-chlorobenzenethiolate. [c] L = 2-phenylbenzenethiolate. [d] L = 2-(*N*-methylcarbamoyl)phenylthiolate.

(s, 2H, N-Meim CH), 7.10 (br, 2H, N-Meim CH), 6.88 (d, 2H, N-Meim CH), 3.65 (s, 6H, N-Meim NMe), 3.55 (s, 18H, NMe_3).

$[Hg(Tab)_2(N\text{-}{}^i Prim)](PF_6)_2$ (6). Compound **6** was prepared as colorless prism crystals in a manner similar to that described for the preparation of **4**, using N-^{i}Prim (0.220 g, 2 mmol) as a starting material. Yield: 0.84 g (90% based on Hg). Anal. Calcd for $C_{24}H_{36}HgF_{12}N_4P_2S_2$: C, 30.82; H, 3.88; N, 5.99. Found: C, 30.98; H, 3.72; N, 5.75. IR (KBr disk): 1623 (w), 1578 (w), 1488 (s), 1410 (m), 1278 (w), 1231 (m), 1122 (m), 1094 (m), 1011 (m), 959 (m), 836 (s), 664 (m), 558 (s) cm^{-1}. UV−vis [MeCN; λ_{max}, nm (ϵ, M^{-1} cm^{-1})]: 280 (85 900). ^{1}H NMR [400 MHz, $(CD_3)_2SO$]: δ 7.58−7.72 (m, 8H, Ph), 7.69 (s, 1H, N-^{i}Prim CH), 7.24−7.26 (d, 1H, N-^{i}Prim CH), 6.88 (d, 1H, N-^{i}Prim CH), 4.43−4.35 (m, 1H, N-^{i}Prim NCH), 3.53 (s, 18H, NMe_3), 1.37−1.38 (m, 6H, N-^{i}Prim CMe_2).

$[Hg(Tab)_2(en)](PF_6)_2\cdot 0.5MeCN$ (7). To a solution of **1** (0.825 g, 1 mmol) in DMF (1 mL) and MeCN (5 mL) was added a solution of en (0.120 g, 2 mmol) in MeOH (8 mL). A workup similar to that used for the isolation of **4** produced colorless blocks of **7**, which were collected by filtration, washed with Et_2O, and dried in vacuo. Yield: 0.77 g (85% based on Hg). Anal. Calcd for $C_{21}H_{35.5}HgN_{4.5}S_2F_{12}P_2$: C, 27.85; H, 3.95; N, 6.96. Found: C, 27.57; H, 3.83; N, 6.86. IR (KBr disk): 3376 (w), 3310 (w), 1591 (m), 1489 (s), 1413 (m), 1314 (w), 1127 (m), 1098 (w), 1010 (m), 958 (w), 837 (s), 743 (w), 558 (s) cm^{-1}. UV−vis [MeCN; λ_{max}, nm (ϵ, M^{-1} cm^{-1})]: 257 (107 500). ^{1}H NMR [400 MHz, $(CD_3)_2SO$]: δ 7.47−7.60 (m, 8H, Ph), 3.52 (s, 18H, NMe_3), 3.15 (br, 4H, NH_2), 2.64 (br, 4H, NCH_2CH_2N).

$[Hg(Tab)_2(eten)](PF_6)_2\cdot 0.5MeCN$ (8). Compound **8** was prepared as colorless blocks in a manner similar to that described for the preparation of **7**, using eten (0.180 g, 2 mmol) as a starting material. Yield: 0.77 g (83% based on Hg). Anal. Calcd for $C_{23}H_{39.5}HgF_{12}N_{4.5}S_2P_2$: C, 29.58; H, 4.26; N, 6.75. Found: C, 29.71; H, 4.55; N, 6.38. IR (KBr disk): 3372 (w), 3325 (w), 1587 (m), 1490 (s), 1415 (m), 1312 (w), 1127 (m), 1011 (m), 958 (m), 843 (s), 746 (w), 558 (s) cm^{-1}. UV−vis [MeCN; λ_{max}, nm (ϵ, M^{-1} cm^{-1})]: 259 (122 700). ^{1}H NMR [400 MHz, $(CD_3)_2SO$]: δ 7.47−7.61 (m, 8H, Ph), 3.52 (s, 18H, NMe_3), 3.43 (br, 3H, NH_2 and NH), 2.73 (m, 2H, CH_3CH_2), 2.58 (br, 4H, NCH_2CH_2N), 1.03−1.06 (m, 3H, CH_3CH_2).

$[Hg(Tab)_2(tmen)](PF_6)_2$ (9). Compound **9** was prepared as colorless plates in a manner similar to that described for the preparation of **7**, using tmen (0.232 g, 2 mmol) as a starting material. Yield: 0.77 g (82% based on Hg). Anal. Calcd for $C_{24}H_{42}HgN_4S_2F_{12}P_2$: C, 30.62; H, 4.50; N, 5.95. Found: C, 30.85; H, 4.33; N, 5.79. IR (KBr disk): 1587 (w), 1491 (s), 1471 (s), 1415 (m), 1293 (w), 1130 (m), 1011 (m), 954 (m), 838 (s), 745 (w), 558 (s) cm^{-1}. UV−vis [MeCN; λ_{max}, nm (ϵ, M^{-1} cm^{-1})]: 258 (88 000). ^{1}H NMR [400 MHz, $(CD_3)_2SO$]: δ 7.49−7.66 (m, 8H, Ph), 3.52 (s, 18H, NMe_3), 2.48 (m, 4H, CH_2), 2.28 (s, 12H, NMe_2).

$[Hg(Tab)_2(dap)](PF_6)_2$ (10). Compound **10** was prepared as colorless blocks in a manner similar to that described for the preparation of **7**, using dap (0.150 g, 2 mmol) as a starting material. Yield: 0.78 g (87% based on Hg). Anal. Calcd for $C_{21}H_{36}HgN_4S_2F_{12}P_2$: C, 28.05; H, 4.04; N, 6.23. Found: C, 28.32; H, 4.24; N, 6.44. IR (KBr disk): 3370 (m), 3307 (w), 1581 (m), 1490 (s), 1310 (w), 1125 (m), 1010 (m), 961 (m), 836 (s), 746 (w), 559 (s) cm^{-1}. UV−vis [MeCN; λ_{max}, nm (ϵ, M^{-1} cm^{-1})]: 264 (85 100). ^{1}H NMR [400 MHz, $(CD_3)_2SO$, ppm]: δ 7.52−7.65 (m, 8H, Ph), 3.53 (s, 18H, NMe_3), 3.23 (br, 4H, NH_2), 2.75 (br, 4H, NCH_2), 1.48−1.53 (m, 2H, CH_2).

$[Hg(Tab)_2(dpt)](PF_6)_2$ (11). Compound **11** was prepared as colorless blocks in a manner similar to that described for the preparation of **7**, using dpt (0.262 g, 2 mmol) as a starting material. Yield: 0.90 g (94% based on Hg). Anal. Calcd for $C_{24}H_{43}HgN_5S_2F_{12}P_2$: C, 30.14; H, 4.53; N, 7.32. Found: C, 30.31; H, 4.25; N, 7.62. IR (KBr disk): 3375 (w), 3310 (w), 1582 (m), 1489 (s), 1414 (m), 1126 (m), 1096 (m), 1010 (m), 957 (m), 837 (s), 744 (w), 558 (s) cm^{-1}. UV−vis [MeCN; λ_{max}, nm (ϵ, M^{-1} cm^{-1})]: 257 (157 500). ^{1}H NMR [400 MHz, $(CD_3)_2SO$]: δ 7.45−7.58 (m, 8H, Ph), 3.52 (s, 18H, NMe_3), 3.48 (b, 5H, NH_2 and NH), 3.45 (m, 12H, CH_2).

X-ray Structure Determinations. Single crystals of **2**−**11** suitable for X-ray analysis were obtained directly from the above preparations. All measurements were made on a Rigaku Mercury CCD X-ray diffractometer by using graphite-monochromated Mo Kα (λ = 0.710 73 Å) radiation. Each crystal was mounted at the top of a glass fiber and cooled at 153 K for **2** and **4**, 173 K for **3**, 133 K for **5**, 193 K for **6**, and 213 K for **7** in a stream of gaseous nitrogen. In the case of **8**−**11**, each measurement was carried out at ambient temperature. Diffraction data were collected in ω mode

Table 4. Crystallographic Data for **2**−**11**

	2	**3**	**4**
chemical formula	$C_{32}H_{42}F_{12}HgN_4O_2P_2S_2$	$C_{31}H_{41}F_{12}HgN_5OP_2S_2$	$C_{28}H_{36}F_{12}HgN_4P_2S_2$
fw	1069.37	1054.36	983.26
cryst syst	monoclinic	triclinic	monoclinic
space group	*C*2/*c*	$P\bar{1}$	*P*2/*c*
a (Å)	17.257(4)	6.0902(12)	17.929(4)
b (Å)	25.198(5)	16.108(3)	6.0177(12)
c (Å)	10.127(2)	19.950(4)	17.734(4)
α (deg)			89.79(3)
β (deg)	106.01(3)	85.98(3)	112.53(3)
γ (deg)			79.55(3)
V (Å^3)	4232.8(17)	1919.8(7)	1767.3(8)
Z	4	2	2
T (K)	153	173	153
D_{calcd} (g·cm^{-3})	1.678	1.824	1.848
μ (cm^{-1})	38.97	42.93	46.54
$2\theta_{max}$ (deg)	50.7	50.7	51.08
no. of reflns collected	20 535	18 953	15 739
no. of unique reflns	3873 (R_{int} = 0.0329)	6988 (R_{int} = 0.0358)	3098 (R_{int} = 0.1598)
no. of obsd reflns	3663 [$I > 2.00\sigma(I)$]	6284 [$I > 2.00\sigma(I)$]	2902 [$I > 2.00\sigma(I)$]
no. of variables	329	495	228
R^a	0.0462	0.0342	0.1055
wR^b	0.1280	0.0608	0.2906
GOF^c	1.092	1.088	1.045

	5	**6**	**7**	**8**
chemical formula	$C_{26}H_{38}F_{12}HgN_6P_2S_4$	$C_{24}H_{36}F_{12}HgN_4P_2S_2$	$C_{42}H_{71}F_{24}Hg_2N_9P_4S_4$	$C_{46}H_{79}F_{24}Hg_2N_9P_4S_4$
fw	989.29	935.22	1811.42	1867.52
cryst syst	triclinic	orthorhombic	monoclinic	monoclinic
space group	$P\bar{1}$	*Fdd*2	*C*2/*c*	$P2_1/n$
a (Å)	5.8189(12)	37.807(8)	38.486(8)	18.777(4)
b (Å)	17.263(3)	57.506(12)	9.3775(19)	8.5461(17)
c (Å)	19.112(4)	6.0684(12)	21.008(4)	23.813(5)
α (deg)	67.23(3)			
β (deg)	89.83(3)		120.54(3)	109.77(3)
γ (deg)	89.33(3)			
V (Å^3)	1770.1(7)	13193(5)	6529(3)	3596.0(15)
Z	2	16	4	2
T (K)	133	193	213	291
D_{calcd} (g·cm^{-3})	1.856	1.883	1.843	1.725
μ (cm^{-1})	46.49	49.82	50.30	45.69
$2\theta_{max}$ (deg)	50.7	50.7	50.0	50.0
no. of reflns collected	17 393	31 920	12 525	16 764
no. of unique reflns	6389 (R_{int} = 0.0522)	5896 (R_{int} = 0.0579)	5687 (R_{int} = 0.0425)	6083 (R_{int} = 0.1080)
no. of obsd reflns	5664 [$I > 2.00\sigma(I)$]	2517 [$I > 2.00\sigma(I)$]	4422 [$I > 2.00\sigma(I)$]	3668 [$I > 2.00\sigma(I)$]
no. of variables	450	406	330	409
R^a	0.0410	0.0398	0.0908	0.1091
wR^b	0.0951	0.1130	0.2395	0.2597
GOF^c	1.055	1.192	1.082	1.067

	9	**10**	**11**
chemical formula	$C_{24}H_{42}F_{12}HgN_4P_2S_2$	$C_{21}H_{36}F_{12}HgN_4P_2S_2$	$C_{24}H_{43}F_{12}HgN_5P_2S_2$
fw	941.29	899.21	956.30
cryst syst	triclinic	triclinic	triclinic
space group	$P\bar{1}$	$P\bar{1}$	$P\bar{1}$
a (Å)	8.3238(17)	10.122(2)	9.0991(18)
b (Å)	14.768(3)	13.077(3)	0.815(2)
c (Å)	15.609(3)	14.296(3)	19.090(4)
α (deg)	67.95(3)	111.01(3)	104.09(3)
β (deg)	89.05(3)	96.34(3)	102.62(3)
γ (deg)	82.53(3)	111.27(3)	92.34(3)
V (Å^3)	1762.2(7)	1582.0(9)	1769.3(7)
Z	2	2	2
T (K)	291	291	291
D_{calcd} (g·cm^{-3})	1.774	1.888	1.795
μ (cm^{-1})	46.63	51.89	46.46
$2\theta_{max}$ (deg)	50.7	50.7	55.7
no. of reflns collected	17 002	15 452	16 721
no. of unique reflns	6396 (R_{int} = 0.0400)	5742 (R_{int} = 0.0372)	6394 (R_{int} = 0.0467)
no. of obsd reflns	2338 [$I > 2.00\ \sigma(I)$]	5269 [$I > 2.00\ \sigma(I)$]	5384 [$I > 2.00\ \sigma(I)$]
no. of variables	344	334	443
R^a	0.0522	0.0415	0.0528
wR^b	0.1336	0.1028	0.1170
GOF^c	1.065	1.039	1.090

^{a} $R = \sum||F_o| - |F_c||/\sum|F_o|$. ^{b} $wR = \{\sum w(F_o^2 - F_c^2)^2/\sum w(F_o^2)^2\}^{1/2}$. ^{c} GOF = $\{\sum w((F_o^2 - F_c^2)^2)/(n - p)\}^{1/2}$, where n = number of reflections and p = total number of parameters refined.

with a detector-to-crystal distance of 35 mm. Cell parameters were refined by using the program *Crystalclear* (Rigaku and MSc, version 1.3, 2001) on all observed reflections. The collected data were reduced by using the program *CrystalClear* (Rigaku and MSc, version 1.3, 2001), and an absorption correction (multiscan) was applied. The reflection data were also corrected for Lorentz and polarization effects.

The crystal structures of **2**−**11** were solved by direct methods and refined on F^2 by full-matrix least squares using anisotropic displacement parameters for all non-H atoms.[24] One Tab ligand in **2** was found to be disordered over two positions with an occupancy factor of 0.525/0.475 for S1/S1A, C1−C9/C1A−C9A, and N1/N1A. The methyl groups of the Tab ligand in **4** were split into two sites with an occupancy ratio of 0.667/0.333 for C7−C9/C7A−C9A. The methyl groups of one Tab ligand and the F atoms of one PF_6^- anion in **11** were split into two sites with an occupancy ratio of 0.43/0.57 for C7−C9/C7A−C9A and F7−F12/F7A−F12A. The H atoms of the NH_2 and NH groups were located from Fourier maps, and their N−H distances of NH_2 were restrained to be equal. The H atom of the hydroxyl group in the MeOH solvent molecule in **2** was also located from Fourier maps. All other H atoms were placed in geometrically idealized positions (C−H = 0.98 Å for methyl groups; C−H = 0.95 Å for phenyl groups) and constrained to ride on their parent atoms with $U_{iso}(H) = 1.5U_{eq}(C)$ for methyl groups and $U_{iso}(H) = 1.2U_{eq}(C)$ for phenyl groups. Important crystal data and collection and refinement parameters for **2**−**11** are summarized in Table 4.

(24) (a) Sheldrick, G. M. *SHELXS-97, Program for Solution of Crystal Structures*; University of Göttingen: Göttingen, Germany, 1997. (b) Sheldrick, G. M. *SHELXL-97, Program for Refinement of Crystal Structures*; University of Göttingen, Göttingen, Germany, 1997.

Acknowledgment. This work was supported by the National Natural Science Foundation of China (Grants 20525101 and 20871088), the State Key Laboratory of Organometallic Chemistry of Shanghai Institute of Organic Chemistry (Grant 08-25), the Qin-Lan Project of Jiangsu Province, and the SooChow Scholar Program and Program for Innovative Research Team of Suzhou University.

Supporting Information Available: Crystallographic data of **2**−**11** (CIF) and views of the hydrogen-bonded networks for **2**−**11**. This material is available free of charge via the Internet at http://pubs.acs.org.

IC8021744